Journal of the Mechanical Behavior of Biomedical Materials 74 (2017) 392–399

Contents lists available at ScienceDirect

Journal of the Mechanical Behavior of Biomedical Materials

journal homepage: www.elsevier.com/locate/jmbbm

Development of a penetration friction apparatus (PFA) to measure the frictional performance of surgical suture

Gangqiang Zhang[a,b,c], Tianhui Ren[c], Walter Lette[b], Xiangqiong Zeng[a,b,*], Emile van der Heide[b,d,e]

[a] Advanced Lubricating Materials Laboratory, Shanghai Advanced Research Institute, Chinese Academy of Sciences, 201210 Shanghai, China
[b] Laboratory for Surface Technology and Tribology, University of Twente, 7500AE Enschede, The Netherlands
[c] School of Chemistry and Chemical Engineering, Key Laboratory for Thin Film and Microfabrication of the Ministry of Education, Shanghai Jiao Tong University, 200240 Shanghai, China
[d] TU Delft, Faculty of Civil Engineering and Geosciences, Stevinweg 1, 2628 CN Delft, The Netherlands
[e] Ghent University, Soete Laboratory, Technologiepark Zwijnaarde 903, B-9052 Zwijnaarde, Belgium

ARTICLE INFO

Keywords:
Penetration friction apparatus (PFA)
Sliding
Friction
Surgical suture
Soft tissue

ABSTRACT

Nowadays there is a wide variety of surgical sutures available in the market. Surgical sutures have different sizes, structures, materials and coatings, whereas they are being used for various surgeries. The frictional performances of surgical sutures have been found to play a vital role in their functionality. The high friction force of surgical sutures in the suturing process may cause inflammation and pain to the person, leading to a longer recovery time, and the second trauma of soft or fragile tissue. Thus, the investigation into the frictional performance of surgical suture is essential. Despite the unquestionable fact, little is actually known on the friction performances of surgical suture-tissue due to the lack of appropriate test equipment.

This study presents a new penetration friction apparatus (PFA) that allowed for the evaluation of the friction performances of various surgical needles and sutures during the suturing process, under different contact conditions. It considered the deformation of tissue and can realize the puncture force measurements of surgical needles as well as the friction force of surgical sutures.

The developed PFA could accurately evaluate and understand the frictional behaviour of surgical suture-tissue in the simulating clinical conditions. The forces measured by the PFA showed the same trend as that reported in literatures.

1. Introduction

The surgical suture is used to suture tissues in surgery operation. The general performance of surgical suture is based on its physical properties and handling characteristics (Dart and Dart, 2011). With respect to the ability to easily penetrate through tissues, the friction force of surgical suture-tissue plays a crucial role. Generally, high friction between surgical sutures and tissues may cause inflammation and pain to the person, leading to a longer recovery time, and the second trauma of soft or fragile tissue (Apt and Henrick, 1976). This phenomenon was particularly evident for multifilament surgical sutures with the twist structure and rough surface. In addition, by providing accurate tribological parameters of surgical sutures during use to the surgeon, the medical risk caused by the selection surgical suture could be balanced, thereby improving the patient's postoperative recovery. Besides, it might provide support for interactive virtual reality, e.g. for a surgical simulator (O'Toole et al., 1999).

The evaluation standard for the frictional behaviour of surgical sutures during suturing has not been established. It was found that few tribological apparatuses have been designed to systematically study the friction behaviour of surgical sutures.

The friction performance of fibrous material has been studied by a number of researchers using three different methods. The first kind of method is an apparatus developed by Tabor D et al. (Tabor, 1957) to determine the friction of crossed fibers in a controllable atmosphere. Roselman I et al. (Roselman and Tabor, 1976) and Thomas (McBride, 1965) investigated the friction between carbon fibers with a similar apparatus. The second kind of method is that two fibers are twisted together and the force required to cause the slippage is measured (Fair and Gupta, 1982). This device can only be used for long fibers. The third kind of method is the classical capstan method (Gao et al., 2015; Robins et al., 1984; Tu and For, 2004a,b), which is regarded as a valuable technological tool for assessing the friction of the fibers when passing over a curved surface of cylindrical body. The capstan method

* Corresponding author at: Advanced Lubricating Materials Laboratory, Shanghai Advanced Research Institute, Chinese Academy of Sciences, 201210 Shanghai, China.
E-mail address: zengxq@sari.ac.cn (X. Zeng).

http://dx.doi.org/10.1016/j.jmbbm.2017.06.031
Received 10 March 2017; Accepted 24 June 2017
Available online 26 June 2017

is used to evaluated the friction performance of surgical suture with different structures (Zhang et al., 2017). These experiments are described in an overview (Yuksekkay, 2009).

The methods mentioned above could not accurately test the penetration friction force when the surgical suture penetrating through tissue. Firstly, the contact condition between surgical sutures and tissues is of surrounding penetration contact condition. The interaction mechanical characteristics of fiber-fiber and fiber-metal contact are different from that of surgical suture-tissue contact. Secondly, the normal load, which is perpendicular to the motion direction, is generated by the resilience deformation of tissue instead of the applied load.

A few researches have investigated the friction force of surgical sutures when penetrating through tissues. George et al. (Rodeheaver, 1983) studied the frictional forces during the coated synthetic absorbable sutures pulled through the skin of the rabbit. Bezwada et al. (Bezwada et al., 1995) estimated the frictional forces during Monocryl[@] suture passing through the surgically prepared posterior dorsal rats skin using an Instron tensile testing machine. Chen et al. (2015) evaluated the handling characteristics of an antibacterial braided silk suture with one equipment. This equipment could test the tissue drag friction resistance of surgical sutures and the fiber-to-fiber friction force. Jarrett et a1. (Jarrett et al., 1994, 1995) described an apparatus for measuring surgical suture friction. A suture was passed through a piece of animal tissue to which a dead weight was attached. The force was measured when the suture moves through the tissue.

Up to now, researchers haven't investigated the friction performances of surgical suture-tissue by simulating the suturing procedure due to the lack of appropriate test equipment. In order to simulate the suturing procedure reasonably, a penetration friction apparatus (PFA) was designed to provide a method for quantifying the force that occurred during the suturing procedure. In addition, this apparatus could measure the forces during surgical needles puncturing tissues and surgical sutures penetrating through tissues. This study was conducted with numerous variables, including the surgical needles, the deformation of tissues.

This paper was organized as follows. Firstly, the composition of the PFA was detailly described. The function and instructions of this equipment were also presented. Subsequently, the puncture forces of surgical needle-tissue were investigated, the penetration friction force of surgical suture-tissue, as well as the effects of tissue deformation and surgical needle size on the friction force during surgical suture penetration procedure.

2. Material preparation and experimental procedure

2.1. Materials preparation

In order to verify the feasibility of PFA, a straight steel stainless tapered needle, a multifilament surgical suture and a kind of skin substitute were used in the experiment.

The straight steel stainless tapered needle with silicon coating, supplied by Weihai Weigao Medical Instruments Co., Ltd., was used in this study. The work of Shergold and Fleck (Shergold and Fleck, 2005) and that of Azar and Hayward (Azar and Hayward, 2008) suggested that the morphology of the crack which is left in the tissue after the needle puncture depends on the shape of needle tip. The tapered needle has a sharp tip with smooth edges and is causes less wear to the surrounding tissues. The silicon-coating of needle body guarantee a minimal resistance to penetration and an optimal passage through the tissue. Furthermore, a hole was drilled along the axial of the needle at the end to attach the surgical suture, as shown in Fig. 1. The surgical needle was laser drilled, which provided a virtually step-free transition from the surgical suture to the needle, thus reducing tissue trauma or wear to the skin substitute. Two type (1# and 4#) of surgical needles were selected. The properties of surgical needles were given in Table 1.

Polyglycolic acid (PGA) multifilament surgical suture, synthetic, absorbable and braided surgical suture, supplied by Weihai Weigao Medical Instruments Co., Ltd. was chosen this study. This suture was used in the surgical operation commonly. The related properties of the PGA multifilament surgical suture were shown in Table 2. In this study, Sil8800 (Red, 80 IRHD), supplied by Superior Seals (Wimborne, Dorset), was chosen as a skin substitute. Its toughness and constitutive response are close to those of skin (Azar and Hayward, 2008; Shergold and Fleck, 2005; Shergold et al., 2006).

The surgical needle and surgical suture were sterilization, and packed with the sterilizing tube by the manufacturer. Before the test, the surgical suture was cut into 25 cm pieces. The circular skin substitute samples with a diameter of 23 mm were cut from a piece of silicon sheet 2 mm thick. The circle skin substitute samples were ultrasonically cleaned in acetone, isopropanol, and finally in water, 10 min for each.

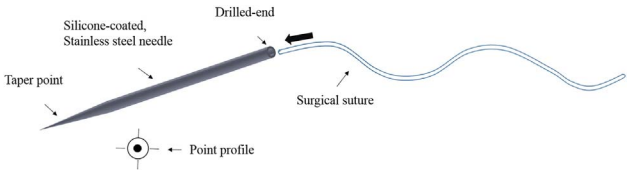

Fig. 1. Needle and surgical suture.

Table 1
Properties of surgical needles.

Type	Diameter (mm)	Length (mm)	Drilled hole diameter (mm)	Needle tip (mm)
1 #	0.86	60	0.55	3
4#	0.51	19	0.25	1.4

Table 2
Properties of surgical sutures.

Surgical suture	Size	Diameter (mm)
PGA Multifilament	2	0.59
	1	0.51
	0	0.46
	2–0	0.34
	3–0	0.23
	4–0	0.19
	5–0	0.13
	6–0	0.08

2.2. Design of penetration friction apparatus

In order to reasonably simulate the suturing procedure (surgical needle puncture and surgical suture penetration) and reliably evaluate the friction performance of surgical sutures, we considered a few aspects from the view of tribology, including the deformation of skin substitute, vertical penetration and the free end of surgical suture.

Skin substitute, as an elastic rubber, often exhibit large deformation when surgical needle pierced it and surgical suture penetrated through it. The rubber deformation was affected by the per-strain in radial direction when surgical needles puncturing through rubber (Nguyen et al., 2009b). In experimental instruments, the effect of the deformation of skin substitute was considered both in the axial and radial directions of surgical needle and suture during the penetration procedure. Firstly, the diameter of the hole in the sample gripper was twice of the surgical needle diameter, meanwhile which was almost four times of surgical suture. This design not only control the deformation of skin in the axial direction of surgical needle, but also guarantee that free space was given for the deformation of skin substitute in the radial direction. Secondly, the force was applied to the sample gripper by the screw to

ensure that the skin substitute was well fixed. The surface of the sample gripper was designed as a rough surface to enhance the friction force in the radial direction. Besides, the deformation of skin substitute caused by applied force which was around the hole wasn't observed.

About the one free end of surgical suture, the surgical suture should penetrate through the skin substitute following the surgical needle puncture track. Therefore, the puncture track of surgical needle directly affected the penetration state of surgical suture. Furthermore, the direction of the pull out force applied on the surgical suture would influence the force distribution to the skin substitute. In this apparatus, the center of the surgical needle (suture) holder and the pull-out point of the surgical needle (suture) in skin substitute were in a vertical line. Thus, the pull out force was perpendicular to the skin surface in the PFA.

In this experiment, one end of the surgical suture was connected to a load cell, and the other end was free. Comparing to the design in the previous study which had a load applied in one end of the surgical suture in the vertical direction (Chen et al., 2015), the design can more reasonably simulate the real suturing condition. It can be explained from the following two aspects. Firstly, the normal load was defined as the load perpendicular to the moving direction of object. Hence, the normal load in the penetration condition was a radial elastic compression force acting on the surface of surgical suture. The load applied in the vertical direction would not affect the normal load. Secondly, due to the motor vibration and the stick-slip phenomenon of surgical suture, the applied load in the previous study would occur elastic beating during the movement. The sloshing of surgical suture in motion would influence the accuracy and reliability of measurement system.

2.3. Experimental procedure

2.3.1. Tribological apparatus configurations

This section provided a description of the penetration friction apparatus (PFA) that was designed to measure the puncture force of surgical needle and the penetration friction force of surgical suture during the suturing procedure. A dedicated experimental sample gripper was designed and manufactured, as shown in Fig. 2a. This sample gripper consisted of three components: sample top holder, sample bottom holder, and fixers (screws). The tissue sample was held between the top and bottom holders which were fixed using the screws. A hole was in the middle of the top and bottom holders respectively, which was called cross hole in this study, for the surgical needle and surgical suture penetrating through the sample gripper. In order to control the deformation of the tissue sample in the puncture and penetration procedure, the diameter of the cross hole could be adjusted to be slightly larger than that of surgical needle.

This sample gripper was assembled in a tensile tester, for instance, the Zwick/Roell 500 N, through an angle adjuster to set the penetration angle between the tissue sample and the surgical needle as shown Fig. 2b. The assemble part was attached to a linear variable differential transformer (LVDT) which could measure the position of the instrument as the connecting rod was moved. All the motions of sample gripper were actuated by stepper motors. Data acquisition from a load cell and the LVDT was realized by the testing software (test Xpert, Zwick) in a computer.

The experimental procedure was divided into two parts as shown in Fig. 3. Firstly, the surgical needle puncturing through the skin substitute, as shown in Fig. 3a. The puncture force was measured by a load cell. Then, the surgical suture connected with a surgical needle and penetrated through the skin substitute following by the surgical needle. Secondly, the surgical suture was cut down from the end of surgical needle, and the cut end of the surgical suture was fixed with the load cell. The opposite end of the surgical suture was free, as shown in Fig. 3b. The friction force of the surgical suture penetrating through the skin substitute was measured during the movement of the sample gripper.

2.3.2. Surgical needle puncture through skin substitute

The sample gripper was assembled in Zwick/Roell tensile tester inversely and moved down following the machine. During the surgical needle punctures through the skin substitute, the ideal motion of the surgical needle is to move in a circular arc about the center (Paris and Rakinic, 2005). On the purpose of reducing uncertainty in the surgical needle mount, in this case, the surgical needle was vertically inserted into a needle clamper which was fixed on a load cell (KAP-S, 50 N) as shown in Fig. 4a. The surgical needle punched into the skin substitute and passed through the cross hole in the middle of the holders as shown Fig. 4b. The load cell measured the puncture force of the surgical needle. Surgical needle insertion rates usually vary between 24 mm/min and 600 mm/min (DiMaio and Salcudean, 2003). In order to reduce noise, perturbation was dominant at a low velocity of 60 mm/min during the surgical needle puncture procedure (Kobayashi et al., 2009). The surgical needle was punctured into the skin substitute sample and stopped after the needle tip penetrated through it totally.

2.3.3. Surgical suture penetration through skin substitute

After the needle punctured through the skin substitute, the surgical suture was glued to the drilled hole at the end of the surgical needle as shown in Fig. 1. The surgical suture penetrated through the skin substitute following the surgical needle. The sample gripper was reversed and assembled in the Zwick/Roell tensile tester again as shown Fig. 5a. One end of the surgical suture was fixed on the holder which connected with the load cell. When the sample gripper moved up following the machine, the load cell measured the force applied to the surgical suture as shown Fig. 5b.

The moving distance of sample gripper was 10 cm. The velocity could be controlled in the range of 50 mm/min to 500 mm/min, which consistent with stitching. To investigate the effect of tissue deformation on friction force, the diameter of the cross hole was adjusted from 0.5 mm to 6 mm. In addition, the different diameter ratios between

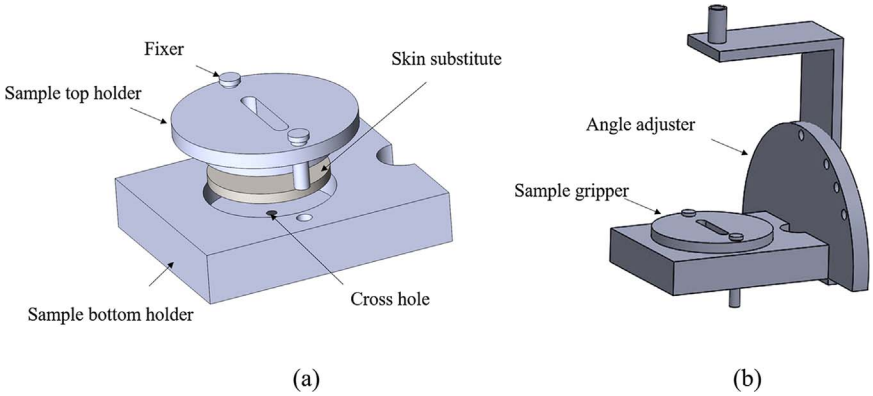

Fig. 2. Friction penetration apparatus. (a) sample gripper, (b) assemble part.

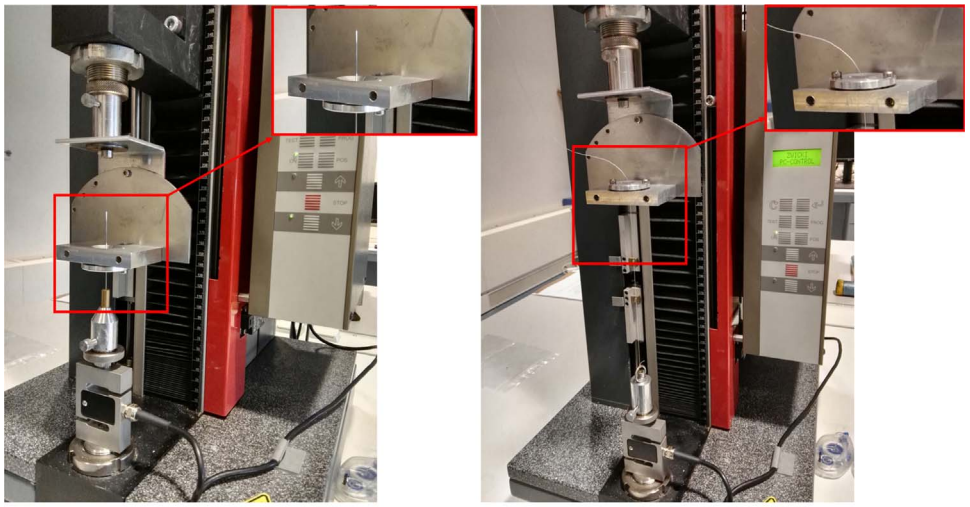

Fig. 3. Image of the experiment process. (a) surgical needle puncture procedure; (b) surgical suture penetration procedure.

surgical needles and sutures ranged from 1.5 to 5.5. An overview of the puncture and penetration test conditions is given in Table 3. Three repetitions of each testing were measured for every experimental setting

2.4. Surface analysis of the material

Keyence VK9710 laser confocal microscope was used to measure the surface topography of the contacting surfaces, i.e. the surgical suture and skin substitute. In this research, the arithmetic mean was used to describe the surface roughness. We measured the roughness (3D, S_a) instead of line roughness (2D, R_a) in order to include the waviness profile of the filament structure.

3. Results and discussion

3.1. Interaction action between surgical needle and skin substitute

The axial force was defined here as the force acting on the surgical needle hub in the direction of insertion. The axial force consisted of puncture force, cutting force, and friction force. Fig. 6 is the axial force-sliding distance curve and the puncture procedure schematic diagram of surgical needle (1 #) interacting with skin substitute at the insertion velocity of 60 mm/min. Five transition points numbered consecutively from A to E during the puncture procedure were shown in Fig. 6a. The trend of this force-sliding distance curve was similar to the result of an alternative method testing surgical needles puncture force (Nguyen et al., 2009a).

Considering the position of a surgical needle relative to the skin substitute boundary, it is possible to distinguish four basic phases: P_1, boundary deformation; P_2, tip insertion; P_3, tip and shaft insertion; P_4, shaft insertion. The schematic diagram of the puncture procedure with the four phases was shown in Fig. 6b.

The first phase (P_1) started when the surgical needle tip contacted with the skin substitute top boundary, and ended when the skin substitute top boundary was breached. As the surgical needle displaces the skin substitute boundary, the load at the surgical needle tip increased. The sliding distance of surgical needle was about 0.4 mm. Once the load exceeded the carrying capacity of skin substitute boundary (Point A in Fig. 6a), a crack would be initiated in the skin substitute and the surgical needle tip started to punch into the skin substitute, which is the starting point of the second phase (P_2). P_2 ended when the needle tip contacted the skin substitute bottom boundary. During this phase, as the surgical needle was advancing, the crack in the skin substitute top boundary was enlarged. The cut made by the edges of the tip was wedged open by the increasing cross-sectional area of the tip (Mueller, 2011). The sliding distance of surgical needle was 1.8 mm (Point C in Fig. 6a) which was approximately equal to the thickness of skin substitute (2 mm). The third phase (P_3) started from Point C, and ended when the skin substitute top boundary was completely crossed by the surgical needle tip. The sliding distance of surgical needle was about 3.2 mm (Point D in Fig. 6a) which was about the length of the surgical

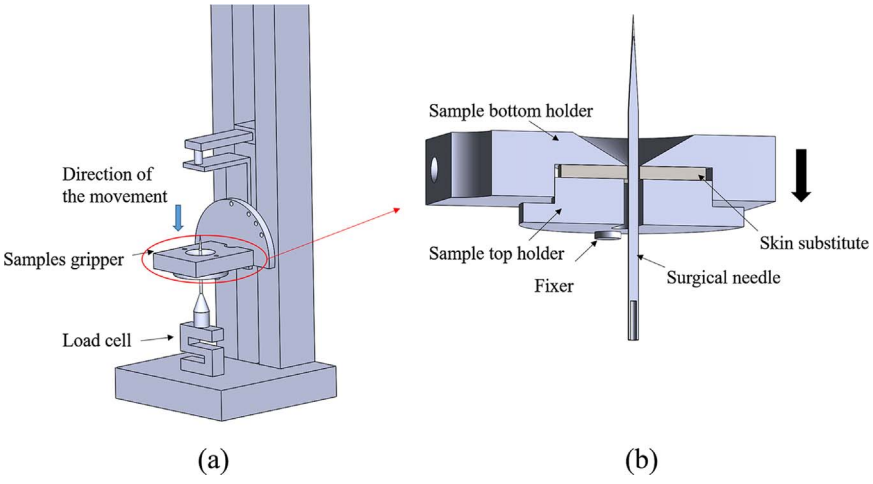

Fig. 4. Surgical needle punctured through skin substitute. (a) A schematic view of the needle puncture through the skin, (b) Profile of the sample gripper during surgical needle puncturing.

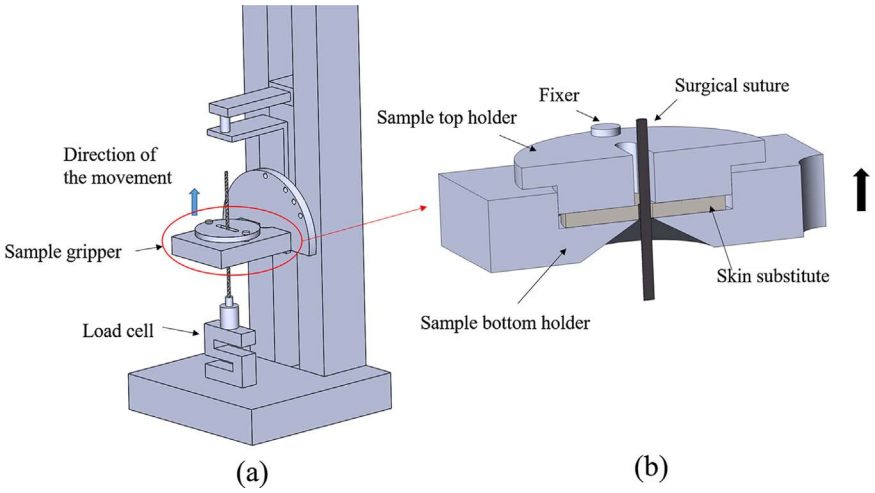

Fig. 5. Surgical suture penetration through skin substitute. (a) A schematic view of the suture penetrated through the skin, (b) Profile of the sample gripper during surgical suture penetrated.

Table 3
Friction test condition.

Test-related Equipment	Instructions Penetration friction apparatus
Diameter of space of gripper	25 ± 0.5 mm
Diameter of cross hole	0.5–6 mm
Puncture angle	90°
Puncture velocity	60 mm/min
Puncture distance	10 mm
Penetration velocity	100 mm/min
Penetration distance	10 cm

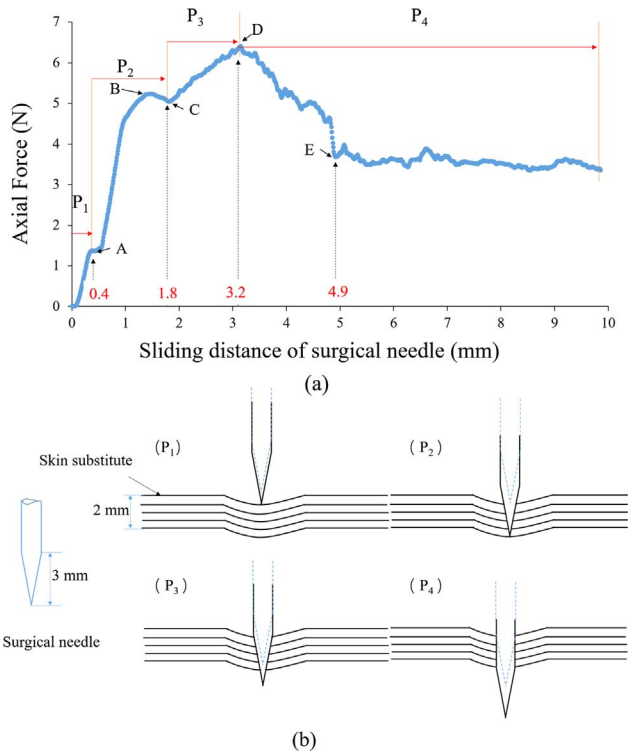

Fig. 6. Surgical needle puncturing skin substitute. (a) axial force-sliding distance relationship of surgical needle; (b) schematic diagram of the puncture procedure.

needle tip (3 mm). During P_3, the crack in the skin substitute bottom boundary was continuously enlarged by the needle tip.

The fourth phase started from the point D when the shaft contacted the skin substitute top boundary. The axial force was decreased with the increasing of the sliding distance of surgical needle (from Point D to E in Fig. 6a). This could be explained as the skin substitute which should be cut became less during the shaft penetrating through the skin substitute. Thus, the cut force of the surgical needle tip decreased as the surgical needle tip punctured out the skin substitute. When surgical needle tip totally penetrated through the skin substitute bottom boundary, the axial force maintained an essentially constant value (Point E in Fig. 6a). This was because only friction force was included in the axial force.

When the surgical needle tip totally penetrated through the skin substitute bottom boundary, the sliding distance was 4.9 mm (point E Fig. 6a) which almost was the sum of the thickness of the skin substitute (2 mm) and the length of the surgical needle tip (3 mm). Similar penetration phases were described in the German industry standard for hypodermic needle tips, DIN 13097.

3.2. Friction force of surgical suture penetrating through skin substitute

The friction force was the pull force measured by PFA during the penetration procedure of surgical suture. That was because both the diameter of surgical needle and the length of planner crack in skin substitute was larger than the diameter of surgical suture. The surgical suture penetrated through skin substitute following the surgical needle pierced track. Consequently, there was no puncture and cutting force when the surgical suture penetrated through the skin substitute.

Fig. 7 shows the friction force – sliding distance curve of PGA multifilament surgical suture (0 #) when penetrating through the skin substitute with the velocity of 100 mm/min following surgical needle (1 #) puncture track. The surgical suture penetration procedure was divided into two phases as shown in Fig. 7. It can be seen that the

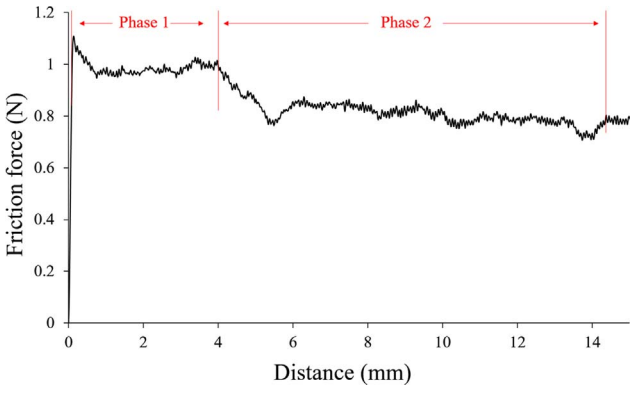

Fig. 7. Friction force of PGA multifilament surgical suture penetrating through skin substitute.

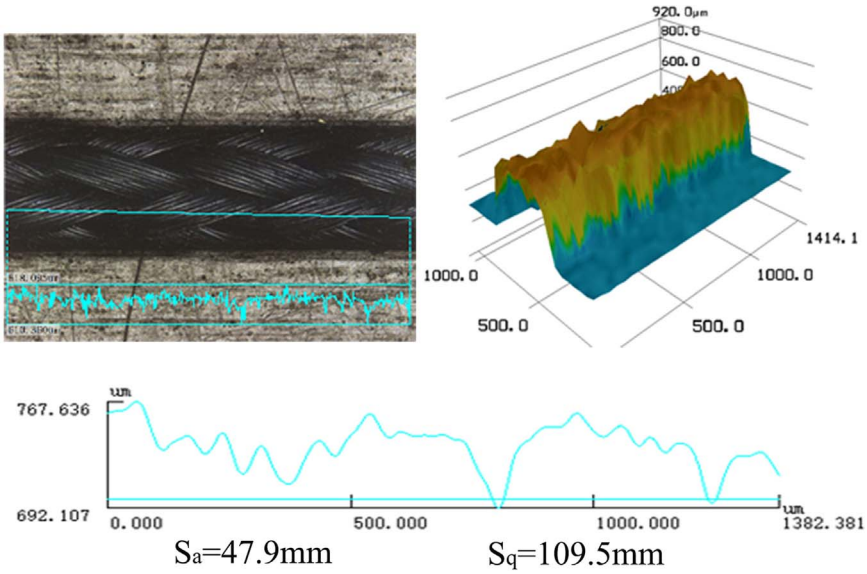

Fig. 8. 0 # PGA multifilament surgical suture. (a) Laser confocal images of the multifilament surgical suture; (b) 3D profile using a confocal microscope; (c) surface parameters.

friction force in Phase 1 was higher than that in Phase 2. That could be explained by the wear phenomenon of skin substitute occurred in the Phase 2.

The surface roughness S_a and S_q of the surgical suture were 47.9 mm and 109.5 mm respectively, as shown in Fig. 8. For multifilament surgical sutures with twisted structure and rough topography, the asperities on the multifilament surgical sutures were formed by the certain regularly twisted fibers. The soft skin substitute was worn by the rough surface of multifilament surgical sutures.

The wear phenomenon was evidenced by Fig. 9. By comparing PGA multifilament surgical suture surfaces before and after friction testing (Fig. 9a and b), it can be seen that the surface of PGA multifilament surgical suture after friction testing adhered the skin substitute wear debris. Fig. 9c shows that the planner crack was closed before the friction test of surgical suture. The same kind of penetration crack was found in a sharp-tipped puncture procedure (Shergold and Fleck, 2005). After the surgical suture penetrated through the crack, some dark area around the planner crack and a gap in the middle of the planner crack were observed, as shown in Fig. 9d. The dark area and the gap were the second trauma caused by the sliding of surgical suture in the penetration procedure. Furthermore, the 3D cross-section profiles of the skin substitute before and after friction testing further revealed the wear of skin substitute (Fig. 9e and f). From Fig. 9e, it can be seen that the punched skin substitute by a surgical needle was irregular rough and staggered together after removing the surgical needle. After the surgical suture sliding, a deeply worn track in the skin substitute was observed as shown in Fig. 9f. This can be explained by the truth that the increasing of the rough of surgical sutures induced to the increasing of contact area, leading to higher friction.

3.3. Effect of the diameter ratio of surgical needle and suture

In this study, the effect of the diameter ratio of the surgical needle and suture on the friction force of surgical suture in the penetration procedure was firstly evaluated. Fig. 10 shows that the friction force of PGA multifilament surgical suture with the diameter ratios of surgical needle and suture varying from 1.5 to 5.5. It can be seen that when the diameter ratio of surgical needle and suture was larger than 2.5, the friction force was almost stable at 0.4 N. When the diameter ratio was smaller than 2.5, the friction force sharply increased up to 1.2 N with the decreasing of the diameter ratio. Therefore, to ensure both less trauma and less friction, optimal diameter ratio of the surgical needle and suture should be 2.5.

3.4. Effect of the diameter of cross hole

Fig. 11 shows the friction force with different diameters of the cross hole in the sample gripper (from 0.5 mm to 6 mm) when the PGA multifilament surgical suture (0#) penetrated through skin substitute following the surgical needle (1#) puncture track. It can be seen that the friction force increased with the increasing of the diameter of the cross hole in both Phase 1 and Phase 2. That was because the diameter of the cross hole affected the deformation of the skin substitute, subsequently, affected the friction force.

Fig. 12 shows the state of the surgical suture inserted through the skin substitute with and without of the pull force. The distance (d) increased with the increasing of the hole diameter as shown in Fig. 12a. The holding force transferred to surgical suture by the skin substitute in the radial direction decreased with the increasing of d. That was to say, the pre-strain decreased with the increasing of the cross hole diameter. The friction force decreased with the increasing of the pre-strain. The similar phenomenon found by Nguyen et al. (Nguyen et al., 2009b) and Figge & Barnet (Figge and Barnett, 1948). Therefore, the increasing of the friction force could be explained by the deformation of skin substitute in the pull-in boundary when the surgical suture was pulled out. More deformation of the elastic skin substitute in radial direction was generated (Fig. 12b) with larger diameter of cross hole. With the increasing of skin deformation, the normal load increased. The effect of skin substitute deformation on the friction force in the surgical suture penetration process was firstly investigated by PFA.

4. Conclusion

The newly developed PFA consisted of the sample gripper and the penetration angle adjuster. It is appropriate for the evaluation of the friction performances of various surgical needles and sutures during the suturing process, under different contact conditions. Penetration experiments on skin substitute with multifilament PGA surgical suture have been performed. The puncture force of surgical needle measured with PFA followed the same trend as that reported in existing research. The friction force-sliding distance relationship of surgical suture demonstrates that the friction force decreased to an essentially constant value in Phase 2 of penetration procedure as the sliding friction and wear of skin substitute. Experiment results reveal that the diameter ratio of surgical suture and needle and the diameter of cross hole influenced the deformation of skin substitute, thereby influencing the friction performance of surgical suture. The optimal diameter ratio of the surgical needle and suture should be 2.5. The PFA provides a

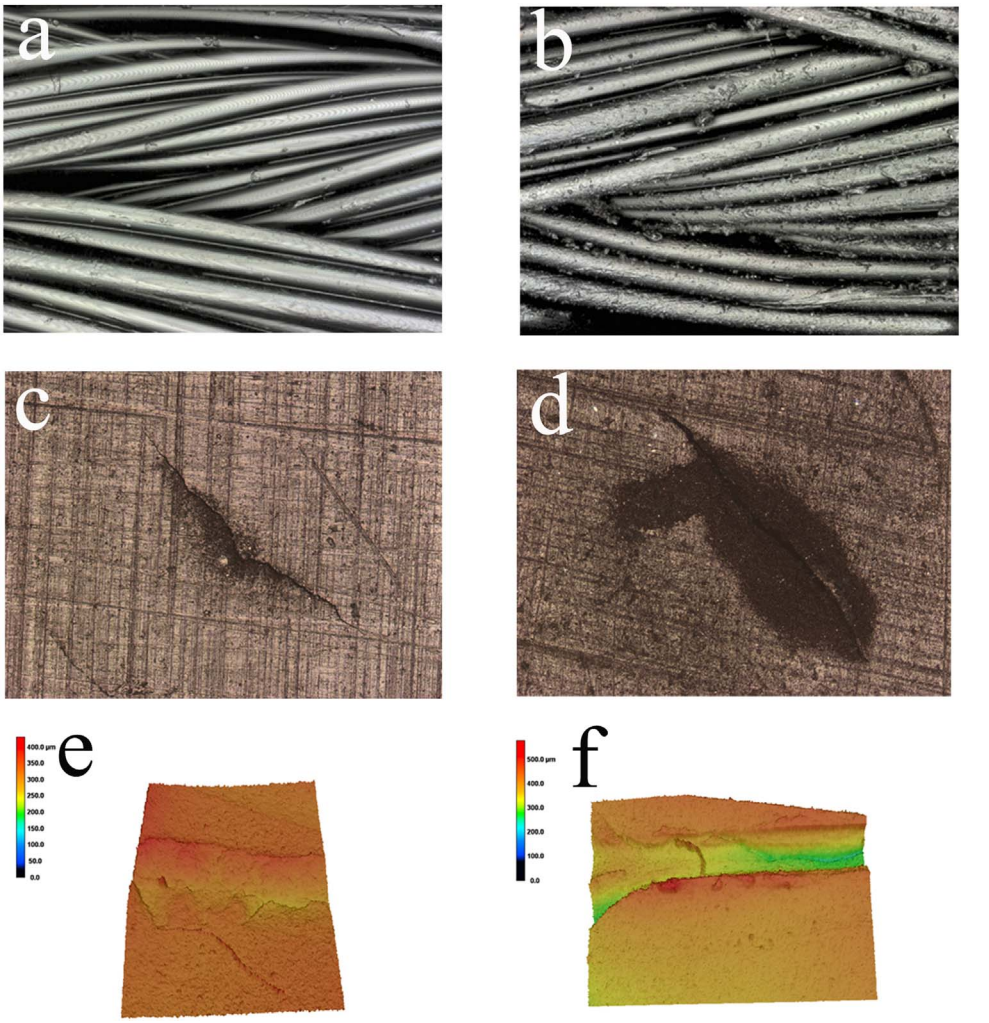

Fig. 9. Topography of surgical suture and skin substitute. (a) surgical suture before friction testing, (b) surgical suture after friction testing, (c) surface topography of skin substitute before friction testing, (d) surface topography of skin substitute after friction testing, (e) 3D cross-section profile of skin substitute sliding contact with surgical needle, (f) 3D cross-section profile of skin substitute sliding contact with the surgical suture.

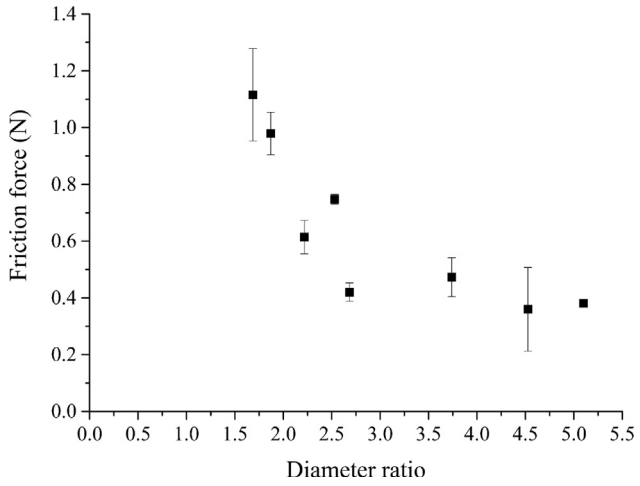

Fig. 10. Friction force of PGA multifilament surgical suture sliding with skin substitute in different diameter ratios of surgical needle and suture.

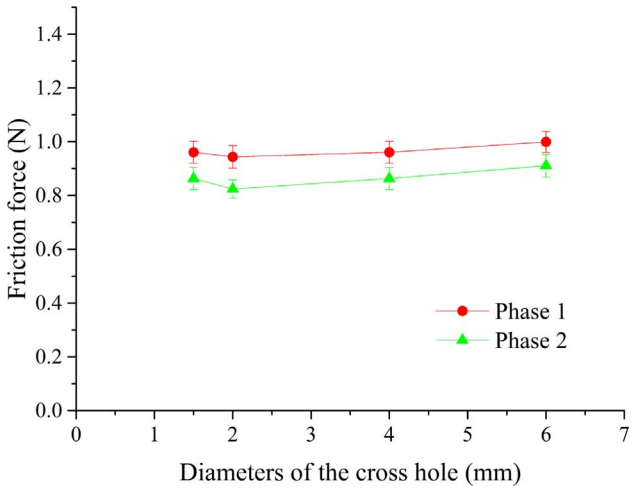

Fig. 11. Friction force of PGA multifilament surgical suture sliding with different diameters of the cross hole in the sample gripper.

convenient and reliable approach to simulate the suturing procedure and study the tribological properties of surgical needle and suture.

Acknowledgements

The authors would like to acknowledge Erik de Vries for his attention and assistance. The present work has been possible thanks to Marie Curie CIG (Grant no. PCIG10-GA-2011-303922); the Shanghai Natural Science Foundation (Grant no. 17ZR1442100); the Shanghai Municipal "Science and Technology Innovation Action Plan" International Cooperation Project (no. 15540723600) for the financial support.

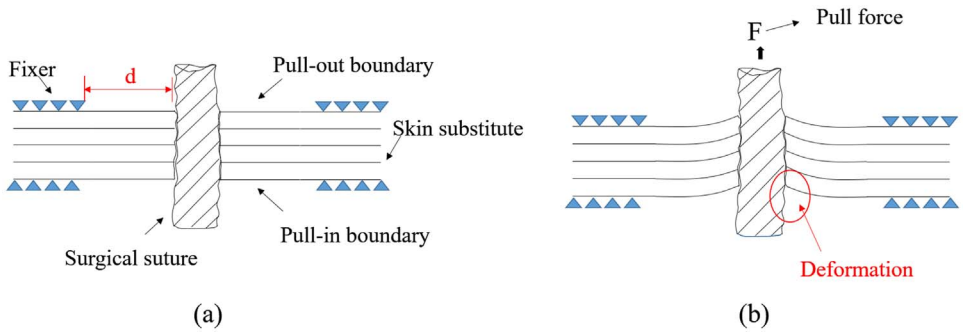

Fig. 12. Event on surgical suture penetrated the skin substitute. (a) surgical suture inserted in the skin substitute; (b) surgical suture penetrated through the skin substitute.

References

Apt, L., Henrick, A., 1976. "Tissue-drag" with polyglycolic acid (Dexon) and polyglactin 910 (Vicryl) sutures in strabismus surgery. J. Pediatr. Ophthalmol. 13, 360–364.

Azar, T., Hayward, V., 2008. Estimation of the Fracture Toughness of Soft Tissue from Needle Insertion, International Symposium on Biomedical Simulation. Springerpp. 166–175.

Bezwada, R.S., Jamiolkowski, D.D., Lee, I.-Y., Agarwal, V., Persivale, J., Trenka-Benthin, S., Erneta, M., Suryadevara, J., Yang, A., Liu, S., 1995. Monocryl® suture, a new ultra-pliable absorbable monofilament suture. Biomaterials 16, 1141–1148.

Chen, X., Hou, D., Tang, X., Wang, L., 2015. Quantitative physical and handling characteristics of novel antibacterial braided silk suture materials. J. Mech. Behav. Biomed. Mater. 50, 160–170.

Dart, A.J., Dart, C.M., 2011. Suture Material: Conventional and Stimuli Responsive. 573-587.

DiMaio, S.P., Salcudean, S.E., 2003. Needle insertion modeling and simulation. IEEE Trans. Robot. Autom. 19, 864–875.

Fair, N., Gupta, B.S., 1982. Effects of chlorine on friction and morphology of human hair. J. Soc. Cosmet. Them. 33, 229–242.

Figge, F., Barnett, D., 1948. Anatomic evaluation of a jet injection instrument designed to minimize pain and inconvenience of parenteral therapy. Am. Pract. Dig. Treat. 3, 197–206.

Gao, X., Wang, L., Hao, X., 2015. An improved Capstan equation including power-law friction and bending rigidity for high performance yarn. Mech. Mach. Theory 90, 84–94.

Jarrett, P.K., Jessup, G., Rosati, L., Martin, C., Maney, J.W., 1994. Coating for tissue drag reduction. Google Pat.

Jarrett, P.K., Jessup, G., Rosati, L., Martin, C., Maney, J.W., 1995. Coating for tissue drag reduction. Google Pat.

Kobayashi, Y., Sato, T., Fujie, M.G., 2009. Modeling of friction force based on relative velocity between liver tissue and needle for needle insertion simulation. In: Proceedings of the Annual International Conference of the IEEE Engineering in Medicine and Biology Society, EMBC. pp. 5274–5278.

McBride, T.E., 1965. Development of an Instrument to Measure Friction of Textile Fibers.

Mueller, F., 2011. Biomechanical test report on hsw fine-ject needles. Technical Report.

Nguyen, C.T., Vu-Khanh, T., Dolez, P.I., Lara, J., 2009a. Puncture of elastomer membranes by medical needles. Part I: mechanisms. Int. J. Fract. 155, 75–81.

Nguyen, C.T., Vu-Khanh, T., Dolez, P.I., Lara, J., 2009b. Puncture of elastomer membranes by medical needles. Part II: mechanics. Int. J. Fract. 155, 83–91.

O'Toole, R.V., Playter, R.R., Krummel, T.M., Blank, W.C., Cornelius, N.H., Roberts, W.R., Bell, W.J., Raibert, M., 1999. Measuring and developing suturing technique with a virtual reality surgical simulator1. J. Am. Coll. Surg. 189, 114–127.

Paris, B., Rakinic, J., 2005. Essential surgical skills. Ann. Surg. 242, 291.

Robins, M.M., Rennell, R.W., Arnell, R.D., 1984. The friction of polyester textile fibres. J. Phys. D: Appl. Phys. 17, 1349–1360.

Rodeheaver, G.T., 1983. Knotting and handling characteristics of coated synthetic absorbable sutures. J. Surg. Res. 35, 525–530.

Roselman, I., Tabor, D., 1976. The friction of carbon fibres. J. Phys. D: Appl. Phys. 9, 2517.

Shergold, O.A., Fleck, N.A., 2005. Experimental investigation into the deep penetration of soft solids by sharp and blunt punches, with application to the piercing of skin. J. Biomech. Eng. 127, 838–848.

Shergold, O.A., Fleck, N.A., Radford, D., 2006. The uniaxial stress versus strain response of pig skin and silicone rubber at low and high strain rates. Int. J. Impact Eng. 32, 1384–1402.

Tabor, D., 1957. Friction, lubrication and wear of synthetic fibres. Wear 1, 5–24.

Tu, C.-F., For, T., 2004a. A study of fiber-capstan friction. 1. Stribeck curves. Tribology Int. 37, 701–710.

Tu, C.-F., For, T., 2004b. A study of fiber-capstan friction. 2. Stick–slip phenomena. Tribology Int. 37, 711–719.

Yuksekkay, M.E., 2009. More about fibre friction and its measurements. Text. Progress 41, 141–193.

Zhang, G., Ren, T., Zeng, X., van der Heide, E., 2017. Influence of surgical suture properties on the tribological interactions with artificial skin by a capstan experiment approach. Friction 1–12.